ARTICLE

Molecular consequences of *PQBP1* deficiency, involved in the X-linked Renpenning syndrome

Jérémie Courraud[1,2,3,4], Camille Engel[1,2,3,4,14], Angélique Quartier[1,2,3,4,14], Nathalie Drouot[1,2,3,4,14], Ursula Houessou[1,2,3,4], Damien Plassard[1,2,3,4], Arthur Sorlin[5], Elise Brischoux-Boucher[6], Evan Gouy[7], Lionel Van Maldergem[6], Massimiliano Rossi[7,8], Gaetan Lesca[7,8], Patrick Edery[7,8], Audrey Putoux[7,8], Frederic Bilan[9], Brigitte Gilbert-Dussardier[9], Isis Atallah[10], Vera M. Kalscheuer[11], Jean-Louis Mandel[1,2,3,4] and Amélie Piton[1,2,3,4,12,13]✉

Mutations in the *PQBP1* gene (*polyglutamine-binding protein-1*) are responsible for a syndromic X-linked form of neurodevelopmental disorder (XL-NDD) with intellectual disability (ID), named Renpenning syndrome. *PQBP1* encodes a protein involved in transcriptional and post-transcriptional regulation of gene expression. To investigate the consequences of *PQBP1* loss, we used RNA interference to knock-down (KD) *PQBP1* in human neural stem cells (hNSC). We observed a decrease of cell proliferation, as well as the deregulation of the expression of 58 genes, comprising genes encoding proteins associated with neurodegenerative diseases, playing a role in mRNA regulation or involved in innate immunity. We also observed an enrichment of genes involved in other forms of NDD (*CELF2, APC2*, etc). In particular, we identified an increase of a non-canonical isoform of another XL-NDD gene, *UPF3B*, an actor of nonsense mRNA mediated decay (NMD). This isoform encodes a shorter protein (UPF3B_S) deprived from the domains binding NMD effectors, however no notable change in NMD was observed after *PQBP1*-KD in fibroblasts containing a premature termination codon. We showed that short non-canonical and long canonical UPF3B isoforms have different interactomes, suggesting they could play distinct roles. The link between *PQBP1* loss and increase of *UPF3B_S* expression was confirmed in mRNA obtained from patients with pathogenic variants in *PQBP1*, particularly pronounced for truncating variants and missense variants located in the C-terminal domain. We therefore used it as a molecular marker of Renpenning syndrome, to test the pathogenicity of variants of uncertain clinical significance identified in *PQPB1* in individuals with NDD, using patient blood mRNA and HeLa cells expressing wild-type or mutant *PQBP1* cDNA. We showed that these different approaches were efficient to prove a functional effect of variants in the C-terminal domain of the protein. In conclusion, our study provided information on the pathological mechanisms involved in Renpenning syndrome, but also allowed the identification of a biomarker of *PQBP1* deficiency useful to test variant effect.

Molecular Psychiatry; https://doi.org/10.1038/s41380-023-02323-5

INTRODUCTION

More than a dozen of pathogenic variants, mostly truncating, have been described in *PQBP1* (polyglutamine-binding protein 1) as responsible for syndromic X-linked neurodevelopmental disorders (XL-NDD) with intellectual disability (ID) (Renpenning, Sutherland-Haan, Hamel, Porteous, and Golabi-Ito-Hall) [1–4] regrouped now under the unique term of Renpenning syndrome [5]. Clinical manifestations associated with these neurodevelopmental syndromes include ID, microcephaly, growth retardation, lean body and specific facial features [6].

PQBP1 encodes a protein involved in different cellular processes such as regulation of transcription, splicing, translation or even response to retroviral infection. PQBP1 was initially described as a protein interacting with polyglutamine tracts of huntingtin or ataxin1, through its polar amino-acid-rich domain (PRD) [7]. PQBP1 possesses a nuclear localization signal (NLS) allowing its addressing to the nucleus through the Kapβ2 receptor [8, 9]. In the nucleus, PQBP1 is involved in transcription regulation through its interaction with activated RNA polymerase II [7] and various transcription factors, and in splicing regulation [10]. A WW domain, on the N-terminal side of PQBP1, has a transcriptional activity and interacts with the splicing factor SIPP1 alias WP11. The C-terminal part of PQBP1 includes a domain (CTD) interacting with other splicing factors such as U5-15kDa alias TXNL4A [11]. In the cytoplasm, PQBP1 can be localized in stress granules [12] and was shown to play a role in translation of messenger RNAs [13],

[1]Institut de Génétique et de Biologie Moléculaire et Cellulaire, Illkirch, France. [2]Centre National de la Recherche Scientifique, UMR7104, Illkirch, France. [3]Institut National de la Santé et de la Recherche Médicale, U964 Illkirch, France. [4]Université de Strasbourg, 67 400 Illkirch, France. [5]National Center of Genetics, Laboratoire national de santé, Dudelange, Luxembourg. [6]Centre de Génétique Humaine, CHU Besançon, Université de Franche-Comté, 25056 Besançon, France. [7]Genetics Department, University Hospital of Lyon, Bron 69500, France. [8]Equipe GENDEV, CRNL, Inserm U1028, CNRS UMR 5292, UCB Lyon1, Illkirch, France. [9]Service de génétique médicale, CHU de Poitiers, 86 000 Poitiers, France. [10]Department of Medical Genetics, Lausanne University Hospital and University of Lausanne, Lausanne, Switzerland. [11]Max Planck Institute for Molecular Genetics, Berlin, Germany. [12]Genetic diagnosis laboratory, Strasbourg University Hospital, 67 090 Strasbourg, France. [13]Institut Universitaire de France, Paris, France. [14]These authors contributed equally: Camille Engel, Angélique Quartier, Nathalie Drouot. ✉email: apiton@unistra.fr

Received: 12 January 2023 Revised: 18 October 2023 Accepted: 13 November 2023
Published online: 29 November 2023

notably by binding the elongation factor eEF2 via its WW domain. Loss of *PQBP1* leads to an increase of the phosphorylation of eEF2 stopping translational elongation and resulting in a global decrease of protein synthesis, which affect protein synthesis-dependent synaptic plasticity in the hippocampus [13]. PQBP1 is also involved in the regulation of neuronal ciliogenesis via its interaction with Dynamin2 [14]. Finally, PQBP1 can also play a role in response to retroviral infection, interacting with reverse-transcribed HIV-1 DNA, probably through its CTD domain, and to the viral DNA sensor cGAS probably through its WW domain, and therefore contributing to the innate immune response [15].

In humans, most of the variants described as causing ID are small indels, located in the AG hexamer of exon 4 or downstream, resulting in truncated proteins lacking their C-terminal domain, and few additional truncating variants were also reported [6, 16–18]. Only a unique missense variant (p.Tyr65Cys) was considered as pathogenic for years, reported in a family with severe clinical manifestations classified as Golabi-Ito-Hall syndrome at that time [4]. This missense variant affects a very conserved amino acid position located in the WW domain and disrupts the interaction between PQBP1 and the splicing factor WBP11 leading to a decreased pre-mRNA splicing efficiency [19]. Two other missense variants (p.Arg243Trp and p.Pro244Leu), located in the CTD domain, were identified more recently in patients with ID by our group and others [20, 21] and were considered as likely pathogenic as they were shown to disrupt the binding with the splicing factor TXNL4A [9, 22].

Different animal models of *Pqbp1* loss have been generated, including mice, Drosophila, nematode and Xenopus [23–27]. Constitutive knock-out of *Pqbp1* in mice appears to be lethal (www.mousephenotype.org/), mouse models where *Pqbp1* was knocked-down (~50%) display abnormal anxiety-related behavior, and a decrease in anxiety-related cognition [25]. Nestin-Cre neural-tissue-specific conditional knock-out (*Pqbp1* cKO) display abnormal anxiety-related behavior, as well as abnormal fear conditioning and motor dysfunction at the rotarod test [26]. Recently, the same group demonstrated that cKO mice showed a short stature and a reduction in bone mass, and displayed impairment in bone formation and chondrocyte deficiency with reduced osteoblast and chondrocyte-related gene expression [28]. The *Pqbp1* cKO showed reduced head size, probably resulting from an elongated cell cycle of neural progenitors [26], consistent with the microcephaly described in patients. All these studies have led to a better understanding of the different roles of *Pqbp1*, but no studies have been performed to decipher the consequences of *PQBP1* loss on human neuronal cells.

We describe in this study the consequences of *PQBP1* deficiency in human neural stem cells (hNSC) where *PQBP1* was knocked-down (KD) using siRNA. We report a deregulation of 58 genes, with an enrichment of genes known to cause ID when mutated, as well as the increase of expression of a non-canonical isoform of the *UPF3B* gene, another XL-NDD gene playing a role in nonsense-mediated mRNA decay (NMD) and regulation of translation. While the consequences of this increase and its involvement in the pathophysiology of Renpenning syndrome remain unclear, we showed that we can use it as a biomarker for this form of XL- NDD, in particular to test the pathogenicity of variants of uncertain clinical significance (VUS).

MATERIAL AND METHODS

Plasmids, siRNA and antibodies

A pool of 4 different siRNA directed against *PQBP1* mRNA was used for the KD (1: UGACAGGGAUCGAGAGCGU; 2: AGCCAUGACAAGUCGGACA; 3: ACGAUGAUCCUGUGGACUA; 4: AGAUCAUUGCCGAGGACUA). For complementation test, *PQBP1* inactivation was performed using siRNA n°4. Human *PQBP1* cDNA NM_005710.2 sequence (including the UTR) was subcloned into PCS2+ plasmid under the CMV promoter and optimized to escape to degradation by siRNA n°4 against *PQBP1* by introducing three silent point mutations (c.87 T > A, c.90 C > A and c.96 C > T at positions underlined in siRNA n°4). Benign, pathogenic and VUS variants (Table S1) were introduced by site-directed mutagenesis. Human *UPF3B_L* cDNA (ENST00000276201.7 or NM_080632.2) and *UPF3B_S* (ENST00000636792.1 from ENSEMBL release 106) were subcloned into pcDNA3 plasmid under the CMV promoter and tagged with HA (YPYDVPDYA) at the C-terminal side of the protein. For western blots and immunostaining, specific primary antibodies were used: anti-UPF3B (NSJ BIOREAGENTS), anti-PQBP1 (NOVUSBIO), anti-GAPDH (G9545 Sigma Aldrich). The secondary antibodies used were HRP-labelled goat anti-mouse or anti-rabbit IgG and HRP (Jackson Immunoresearch, Baltimore, PA, USA).

Cell culture, transfection and proliferation assay

Two lines of human neuronal stem cells (hNSC) from male origin were used: hNSC-1 (SA001) and hNSC-2 (GM01869), previously described [29, 30]. They were seeded on poly-ornithine and laminin-coated (Sigma-Aldrich) dishes and maintained in DMEM/F12 and Neurobasal medium (1:1) supplemented with N2, B27, 2-mercaptoethanol (Invitrogen, Carlsbad, CA, USA), BDNF (20 ng/mL), FGF-2 (10 ng/mL)(PeproTech, Rocky Hill, NJ, USA) and EGF (R&D Systems; 10 ng/mL) as described [30]. Lymphoblastoid cell lines (LCL) were previously [1] or newly established by infection of blood lymphocytes using Epstein-Barr virus and were maintained in RPMI without HEPES and 10% fetal calf serum. HEK293 and HeLa cells were maintained respectively in DMEM (1 g glucose / liter), 10% fetal calf serum and gentamicin (40 µg/mL) in CellBind® flasks (Corning, NY, USA) for HEK293T, DMEM (1 g glucose / liter), 5% fetal calf serum and gentamicin (40 µg/mL) in CellBind® flasks (Corning, NY, USA) for HeLa. Cells were transfected using INTERFERin (Polyplus) or Lipofectamine 2000 transfection protocol (Thermo Fisher Scientific) for siRNA and plasmids respectively. Cells were stopped at 24/48 and 96 hours after transfection for protein and RNA extractions. For proliferation assay, reverse transfection of SA001 and GM01869 hNSCs (6400 cells/cm2) was performed in 96-well plates using INTERFERin reagent and 120 nM siRNA according to manufacturer's recommendation. Each day a plate was fixed and stained with DAPI and number of nuclei in each condition counted using CellInsight automated microscope and HCS Studio software (Thermo Fisher Scientific).

Subjects

Lymphoblastoid cell lines (LCL) were available for individuals with pathogenic variants in *PQBP1* ($n = 7$), with variants of uncertain significance ($n = 3$), control individuals ($n = 6$) and individuals with a pathogenic variant in *FMR1* (Fragile X syndrome, FXS) ($n = 4$) (Figure S1, Table S1). Blood RNA samples (PaxGene) were available for individuals with pathogenic variants ($n = 3$) in *PQBP1*, VUS in *PQBP1* ($n = 1$) pathogenic variants in *FMR1* ($n = 2$) and individuals with other genetic forms of ID ($n = 5$, one with a pathogenic variant in *RPS6KA3*, one in *HCN1* and three with no clear molecular diagnosis established). The individuals were referred for genetic testing as part of routine clinical care. The participants or their legal representative signed informed consent for research use (project approved by the Ethics Committee of the Strasbourg University Hospital) as well as authorization for publication. All *PQBP1* variants were named according to the isoform NM_005710.2 which encodes a protein of 265 amino acids. The potential effect of missense variants was predicted using PolyPhen2 (http://genetics.bwh.harvard.edu/pph2/) and CADD (https://cadd.gs.washington.edu/). We collected clinical information for the patients reported for the first time in this study (P7, P8, P9, P10, V2 and V2_s), as well as for the two brothers for whom we previously reported the variant p.Pro244Leu (P2, P2_s)(Table S8).

mRNASeq

Total RNA was extracted 48 h after hNSC transfection. RNA-seq libraries of template molecules suitable for high throughput sequencing were established from 300 ng of total RNA using the KAPA RNA HyperPrep Kit after a first step of purification using poly-T oligo-attached magnetic beads (Roche). Libraries were sequenced on the Illumina Hiseq 4000 sequencer as paired-end 100 base reads. Reads were mapped onto the hg38 assembly of the human genome using Tophat 2.0.10 or 2.0.14 [31] and the bowtie version 2-2.1.0 aligner [32]. Gene expression was quantified using HTSeq-0.6.1 [33], using intersection-nonempty mode and gene annotations from Ensembl release 85. Only non-ambiguously assigned reads were kept. Comparisons of interest were performed using after normalization of read count across libraries with the median-of-ratios method proposed by Anders and Huber and a Wald test was used to estimate the p-values.

Adjustment for multiple testing was performed with the Benjamini and Hochberg method [34]. Alternative splicing and isoform-specific differential expression were identified using DEXSeq 1.14.2 [35], removing the events with less than 5 reads. Only the differences found significant in the si*PQBP1* condition compared to INTERFERin treatment and not with the si*Scramble*, were considered. For the LCL cells, RNA-seq libraries of template molecules were prepared as previously described [30]. The discovery of enriched functional-related gene groups has been performed using DAVID using a background list of 23,600 genes expressed in hNSC (5 reads or more in average obtained in RNaseq data) and a high stringency parameter. Enrichment in genes involved in NDD (SysNDD, may 2022 update) was tested using hypergeometric probability (R package: phyper(overlap-1, list1, population-list1, list2, lower.tail=FALSE).

RT-qPCR

Total RNAs were extracted from cells using the RNeasy extraction kit and treated with RNase free DNAse set during 20 min (Qiagen, Valencia, CA, USA) or from blood using PaxGene blood RNA kit extraction (Preanalytix, Hombrechtikon, Switzerland). RNA levels and quality were quantified using a Nanodrop spectrophotometer and then with a 2100 Bioanalyzer (Agilent, Santa Clara, CA, USA) for the RNA used for RNA-sequencing. For reverse transcription-PCR (RT-PCR), 500 ng to 1 µg of total RNA was reverse transcribed into cDNA using random hexamers and SuperScript IV reverse transcriptase according to manufacturer's recommendation. Real-time PCR quantification (qPCR) was performed on LightCycler 480 II (Roche, Basel, Switzerland) using the QuantiTect SYBR Green PCR Master Mix (Qiagen). All qPCR reactions were performed in triplicate. Primer sets are listed in Table S2. Reaction specificity was controlled by post-amplification melting curve analysis. The relative expression of gene-of-interest *vs GAPDH* and *YWHAZ* was calculated using the 2-(ΔΔCt) method and a parametric Student's t-test was performed in order to compare control vs patient cells or untreated vs siRNA treated cells. Error bars represent standard error of the mean (SEM). All the RNASeq and RT-qPCR experiments are summarized in Figure S1.

Western Blot

Cells were lysed in RIPA buffer supplemented with protease inhibitor cocktail and phosphatase inhibitor cocktail. 5 to 50 µg of protein lysate were separated on 10% SDS-PAGE and transferred to polyvinylidene fluoride membrane. Membranes were blocked in 5% nonfat dry milk diluted in tris buffered saline with tween 20 and probed using the antibodies overnight at 4 °C. GAPDH was used as loading control. Incubation with appropriate secondary HRP-labelled antibody (1 hour at room temperature) was followed by detection with Immobilon western chemiluminescent HRP substrate (Merck Millipore, Darmstadt, Germany).

Immunoprecipitation and Mass Spectrometry analyses

HEK293 were transfected in 6-well plates with 1 µg of pcDNA3 containing the coding sequence of *UPF3B_L* or *UPF3B_S*. Proteins were extracted after 48 hoursand subjected to immunoprecipitation with Pierce Anti-HA Magnetic Beads (Thermofisher 88836) according to manufacturer protocol. Immunoprecipitations were validated by western-blots as previoulsy done [36] before the mass spectrometry analyses (Proteomic platform, IGBMC). Briefly, samples were treated with LysC/Trypsine for liquid digestion and injected in Orbitrap ELITE / C18 Accucore 50 cm (20 µL 0.1%TFA / 1 µL) for 2 h runs in triplicate. Data were processed with Proteome Discoverer 2.2 software using Homosapiens_190716_reviewed. fasta and contaminants_190528.fasta databases. To consider a protein as a candidate interactor, we applied the thresholds to keep only proteins with 1) at least two unique peptides identified, 2) a positive value of Peptide-Spectrum Matching (PSM) in each replicate of the tested condition 3) a positive eXtracted Ion Chromatogram (XIC) value in at least one replicate of the tested condition, 4) a sum of PSM for the three replicates of the control condition (HA-beads only, "Empty") inferior to 5, 5) a sum of PSM for the three replicates of the tested condition (UPF3B_L or UPF3B_L) greater or equal to 5 and 6) a ratio between the Normalized Spectral Abundance Factor (NSAF) of the tested condition (UPF3B_L or UPF3B_L) and the NSAF of the control ("Empty") condition greater or equal to 2.

Measure of nonsense mediated mRNA decay (NMD)

Three fibroblast cell lines carrying heterozygote variants leading to premature stop codon (PTC) in *DYRK1A* (PTC1, NM_001396.4: c.1232dupG, p.Arg413fs), *BRPF1* (PTC2, NM_001003694.1: c.1052_1053del, p.Val351fs) and *CNOT3* (PTC3, NM_014516.3: c.1127_1145del, p.Ala376fs) were used to test the effect of *PQBP1* inactivation or overexpression of UPF3B isoforms on nonsense mediated mRNA decay (NMD). Fibroblasts were cultivated in 6-well-plates and treated during 24 h with the NMD inhibitor emetine (50 µg/ml), si*PQBP1* or pcDNA3-UPF3B_S/UPF3B_L. mRNA were extracted, reverse transcribed, amplified and Sanger sequenced. Quantification of the mutant alleles were performed by calculating the ratio between intensity of peaks corresponding to the mutant vs wilt-type sequences. These ratios were calculated for the different conditions and normalized to emetine treatment (condition without NMD). Comparisons were performed using one-way ANOVA test with Dunnet's correction.

RESULTS

Consequences of *PQBP1* knock-down in human neural stem cells (hNSC)

In order to identify the consequences of *PQBP1* deficiency, we used human neural stem cells (hNSC), which are self-renewal homogenous precursors of cortical neurons representing a relevant model to study pathophysiological mechanisms involved in NDD [30]. We transiently inactivated *PQBP1* in a first line of hNSC (hNSC-1) using specific siRNA and obtained a knock-down (KD) of ~60% of *PQBP1* expression (Fig. 1A, B). As PQBP1 is known to play a role as cell cycle regulator in neural progenitors [26], which is consistent with the microcephaly observed in individuals affected by Renpenning syndrome, we first tested if *PQBP1*-KD affects the proliferation of hNSC. We observed a significant decrease in hNSC proliferation 96 hours after *PQBP1*-KD in hNSC-1 when compared to control condition (transfection agent only) or si*Scramble* (Fig. 1C). A decrease in proliferation, although not reaching statistically significance, was observed for a second line of hNSC from another genetic background (hNSC-2, $p = 0.059$, Figure S2). In order to study the consequences of *PQBP1*-KD on the regulation of gene expression and alternative splicing, we performed bulk RNA sequencing on hNSC-1, which revealed 59 significant differentially expressed protein-coding genes (DEG) in *PQBP1*-KD cells compared to cells treated with transfection agent only (Fig. 1D, Table S3), while no gene was found significantly differentially expressed in the si*Scramble* condition. Unsurprisingly, the most significant DEG was *PQBP1* (log2FC = –0.82, adjusted p-value = *3.7E–8*). Among the other DEG, 46 were down-regulated in *PQBP1*-KD context while only 12 were up-regulated. The down-regulated DEG were enriched in genes known to cause neurodevelopmental disorders (NDD)(9/46 in the "definitive" category from sysNDD database, p-value *2.9E-3*) and in candidate NDD genes (7/46 in the "limited" category from sysNDD database, *p*-value = *1.1E–2*). Pathway analysis revealed six clusters among the DEG: genes encoding i) proteins linked to neurodegenerative diseases including those related to mitochondrial function (*APC2, AMBRA1, MT-CO2, MT-ND3*), ii) RNA-binding proteins involved in mRNA metabolism and regulation of alternative splicing (ex: *CELF2, RBPSM2*), iii) proteins containing LRR repeats (*LRRC61, LRRC4B, LRFN4*), iv) proteins related to innate immunity (*SARM1, PRDM1, N4BP3*), v) transmembrane proteins (*SMIM13, TM4SF18, CPM, NRP1*, etc) and vi) ATP-binding proteins (*DYRK2, CPS1, ABCD1, UHMK1*), however, due to the limited number of DEG identified, the enrichment was not significant after multiple testing corrections (Fig. 1E, Table S4). Decrease in expression of genes encoding enzymes involved in lipid or steroid metabolism *(HSDL2, MID1IP1)* has also been observed. To confirm these changes in gene expression, RT-qPCR was performed on a third serie obtained from hNSC-1 ($n = 3$ samples per condition) as well as on three series of the second hNSC line coming from another genetic background (hNSC-2, $n = 9$ samples per condition in total) (Fig. 1F). Differences in exon coverage were also identified using DEXSeq in 48 protein-coding genes, such as *UPF3B*, *PLXNA2*, *PPP2R5C* or *CHD24* (Table S5, Fig. 2A, Figure S3A). *UPF3B* is, like *PQBP1*, involved in X-linked NDD. The coverage increase detected after *PQBP1*-KD corresponds to an exon of a non-canonical short isoform of *UPF3B* (*UPF3B_S*, ENST00000636792.1) (E'3 in Fig. 2A). This increase was confirmed

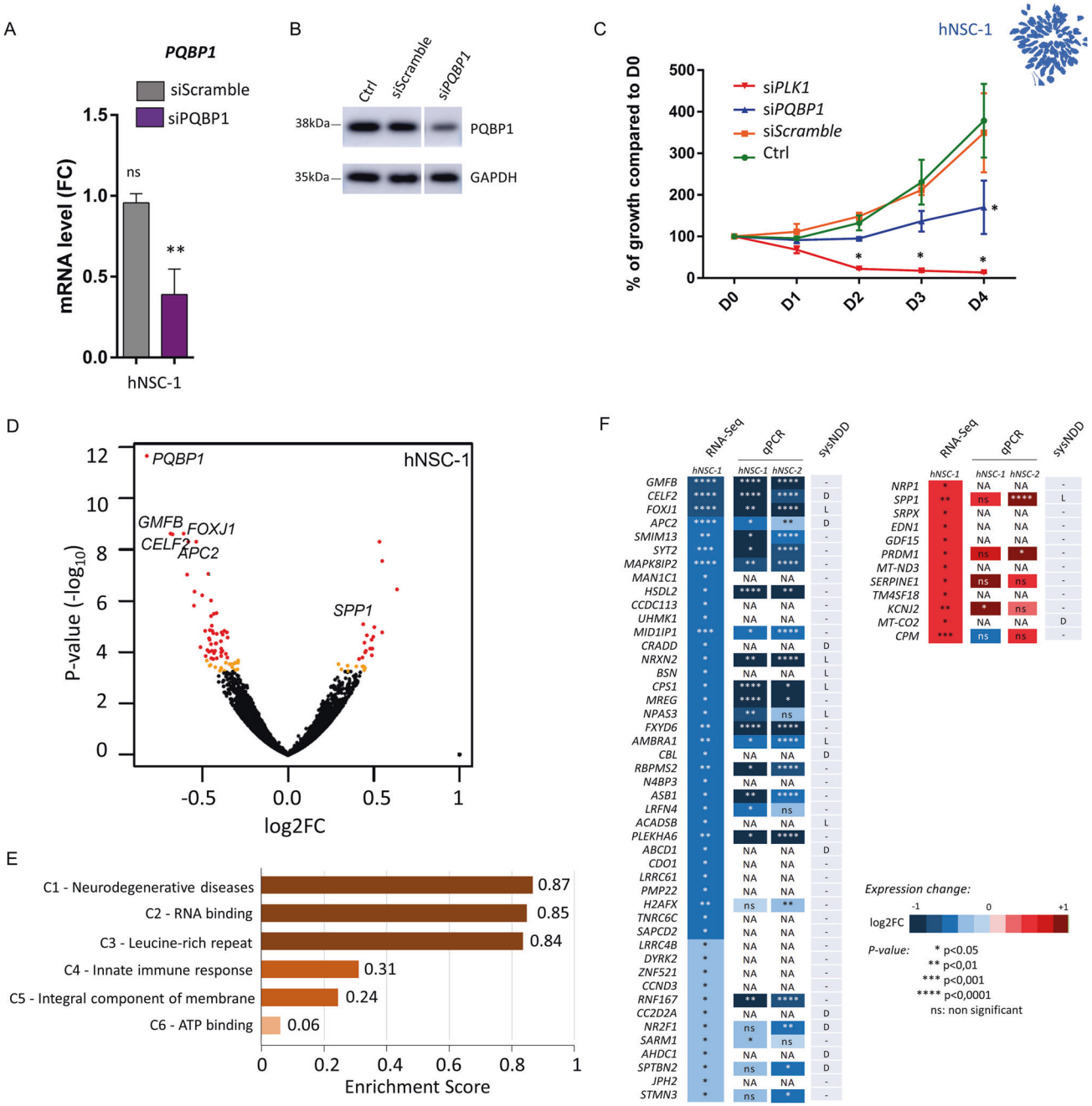

Fig. 1 Consequences of *PQBP1* Knock-Down (KD) in human neural stem cells (hNSC). A RT-qPCR analysis of *PQBP1* mRNA (normalized on *GAPDH* and *YWHAZ*) in hNSC-1 treated using si*Scramble* or *siPQBP1* compared to cells treated with transfectant only (48 h, $n = 3$). Multiple comparison tests were performed using one-way ANOVA test with Dunnet's correction: ns: not significant; ***p*-value < 0.01; Errors bars represent SEM (standard error of the mean). **B** Level of PQBP1 protein extracted from hNSC-1 after 48 h transient *PQBP1*-KD (representative of $n = 3$). **C** Proliferation assay performed on hNSC-1 treated with transfectant alone (Ctrl) or transfected with si*Scramble*, si*PQBP1* or si*PLK1* siRNA (known to induce cell apoptosis). At each time point (day D0, 1, 2, 3, and 4), the number of cells were counted and data normalized with control condition D0 ($n = 3$). Student's t test comparison was done comparing to control: **p*-value < 0.05; Errors bars represent SEM. **D** Volcano plot showing RNA sequencing data (si*PQBP1* vs. Ctrl treated hNSC-1). Genes with no significant change in expression are shown in black; genes deregulated with an adjusted *p*-value between 0.1 and 0.05 are shown in orange while genes significantly top deregulated (adjusted p-value < 0.05, DEG) are shown in red. **E** Clusters of enriched functional-related gene groups identified using DAVID tools among DEG, detailed in Table S4. **F** RT-qPCR analysis of 30 DEG (normalized on *GAPDH* and *YWHAZ*) after *PQBP1*-KD in hNSC-1 (third serie) and in hNSC-2 (3 independent series in triplicates). Genes known to be certainly ("Definitive") or potentially ("Limited") involved in NDD according to the SysNDD database are indicated. Multiple comparison tests were performed using one-way ANOVA test with Dunnet's correction: ns: not significant; **p*-value < 0.01; ***p*-value < 0.01 ****p*-value < 0.001; NA: not tested; expression change is represented in log2FC (blue: increase, red: decrease).

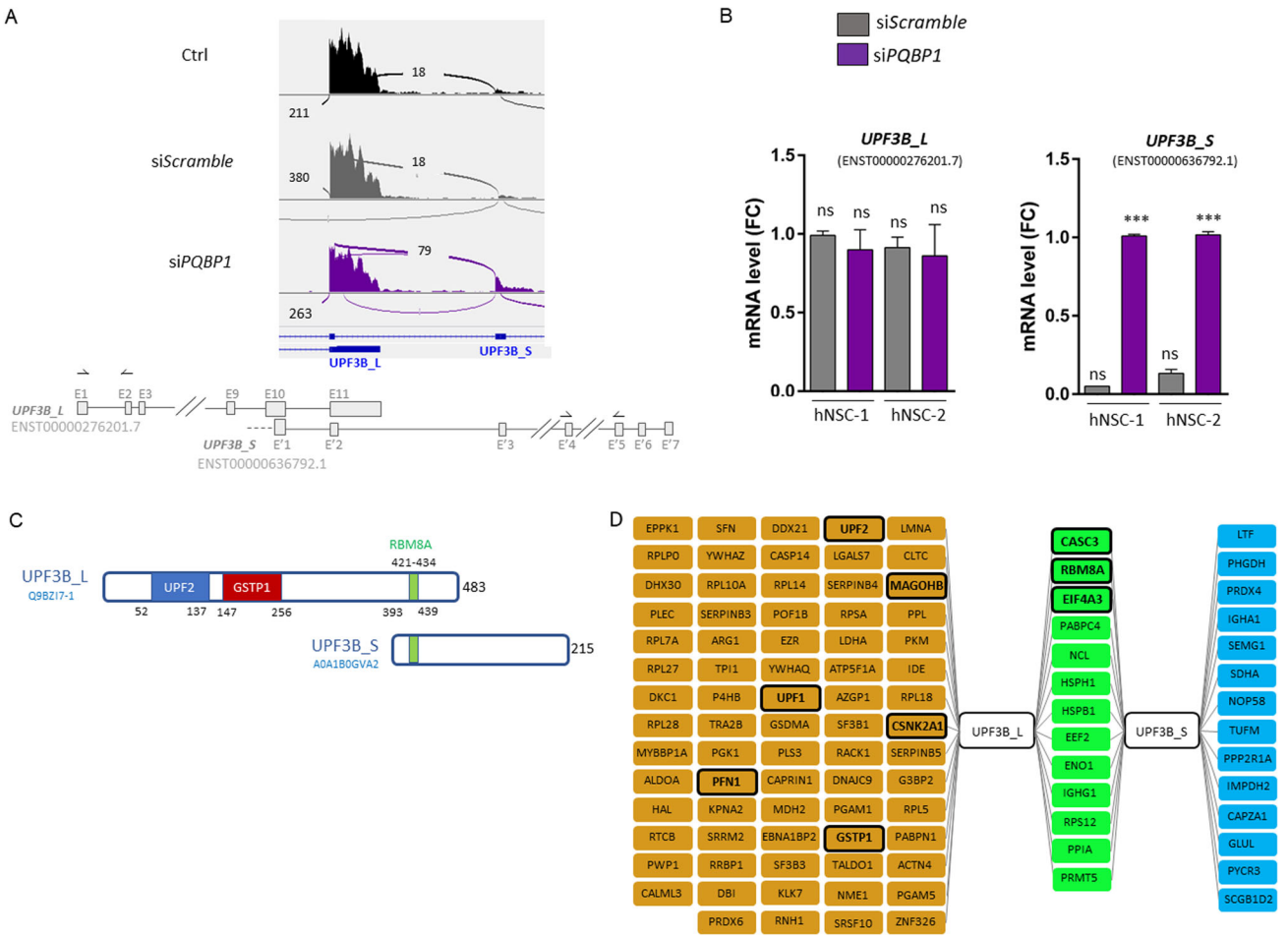

Fig. 2 Expression of a non-canonical isoform of *UPF3B* (*UPF3B_S*) is increased after *PQBP1*-KD. A IGV visualization at the *UPF3B* locus of RNAseq data (Sashimi plot) from hNSC-1 treated with transfectant agent only (Ctrl), siScramble or *PQBP1* siRNA. Exons from the canonical (*UPF3B_L*, ENST00000276201.7) and non-canonical (*UPF3B_S*, ENST00000636792.1) isoforms are represented under the RNASeq reads. The number of reads supporting the E'2-E'3 junction are indicated. qPCR primers used for RT-qPCR validation of *UPF3B_S* and *UPF3B_L* isoforms are represented by black arrows. **B** RT-qPCR analysis of *UPF3B_S* and *UPF3B_L* mRNA levels (normalized on *GAPDH* and *YWHAZ*) in hNSC treated with si*Scramble* or si*PQBP1*. Errors bars represent SEM Multiple comparison tests were performed using one-way ANOVA test with Dunnet's correction: ns: not significant; ****p*-value < 0.001 **C** Schematic representation of UPF3B_L and UPF3B_S proteins with their domains known to interact with UPF2, GSTP1 and RBM8A proteins, Uniprot accession numbers are indicated un light blue. **D** Protein interactome of UPF3B_L and UPF3B_S isoforms characterized by immunoprecipitation coupled to mass spectrometry (IP-MS) after transfection in HEK293 cells. In orange: proteins interacting preferentially with UPF3B_L; in blue: proteins interacting preferentially with UPF3B_S; in green: proteins interacting with both UPF3B_L and UPF3B_S isoforms. Proteins already described as interacting with UPF3B are circled with a black line.

by RT-qPCR in both hNSC-1 and hNSC-2, while no change was observed at the mRNA level for the canonical long isoform (UPF3B_L, ENST00000276201.7) (Fig. 2B).

The increase of *UPF3B_S* expression induced by *PQBP1* knock-down does not affect NMD

UPF3B encodes a protein involved in mRNA nonsense mediated decay (NMD), but the role of *UPF3B_S* is currently unknown. This isoform is particularly expressed in testis but is also expressed at low level in EBV-transformed lymphocytes, in kidney and in different brain region (GTEx database, Figure S4). Therefore, to test if this increase in *UPF3B_S* expression caused by *PQBP1* deficiency affects NMD, we first searched for known NMD target genes [37] among DEG but found no overlap. In parallel, we proceeded to *PQBP1*-KD in fibroblasts carrying a premature truncating variant in other NDD genes (*DYRK1A*, *BRPF1* and *CNOT3*) known to induce transcript degradation by the NMD system [38]. While we were able to confirm the increase of *UPF3B_S* expression after *PQBP1*-KD in fibroblasts, no effect was observed on the level of mutant transcript compared to the untreated condition, suggesting that this has no obvious effect on NMD in fibroblasts (Figure S5). Overexpression of human *UPF3B_L* (ENST00000276201.7) and *UPF3B_S* (ENST00000636792.1) cDNA sequences did not significantly change the NMD level. To better understand the distinct role of UPF3B isoforms, we performed immunoprecipitation-coupled mass spectrometry on proteins extracted from HEK293 cells transfected with these constructs (Fig. 2C). We identified a total of 101 proteins interacting with UPF3B: 13 proteins interacting with both isoforms, 74 proteins interacting preferentially or exclusively with UPF3B_L and only 14 preferentially or exclusively with UPF3B_S (Table S7, Fig. 2D). As expected, we retrieved nine of the known UPF3B interactors annotated in the STRING and BioGRID databases (Fig. 2D) and found that UPF1, UPF2 and ERF3A alias GSPT1 interact only with UPF3B_L but not with UPF3B_S, which lacks the corresponding binding domains (Fig. 2C), while the exon junction complex (EJC)-binding protein RBM8A (alias Y14) interacts with both isoforms. Among the proteins interacting preferentially with UPF3B_S, we identified proteins involved in antibacterial humoral response (LTF, SEMG1, IGHA1) and in redox homeostasis (PRDX4, PHGDH, SDHA).

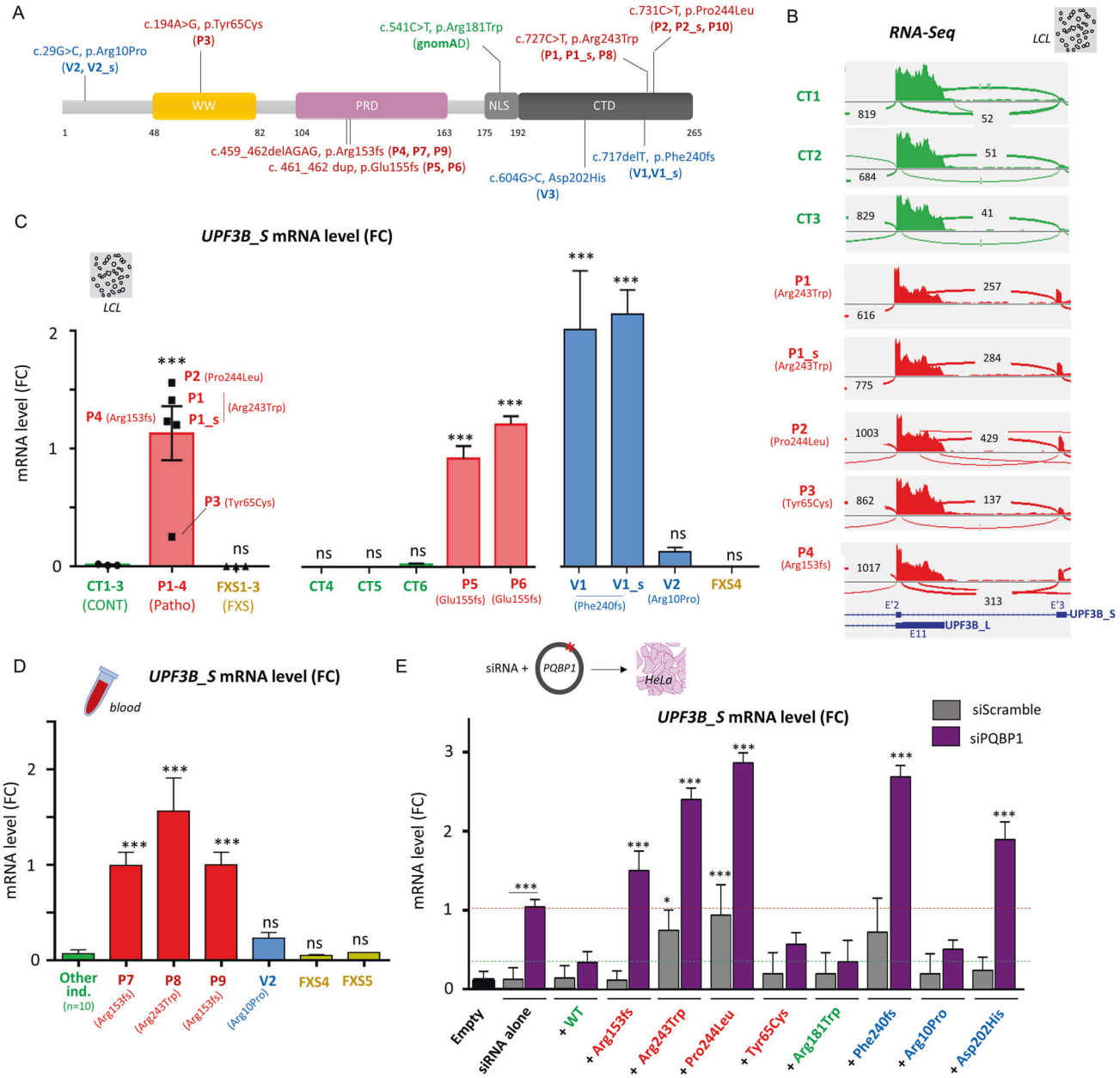

Fig. 3 Increase of *UPF3B_S* is a molecular marker for Renpenning syndrome. A Schematic representation of PQBP1 protein with its different domains (WW: WW domain, PRD: Proline-rich domain, NLS: nuclear localization signal, CTD :C-terminal domain) and the different variants analyzed in this study: in green, a missense variant found in males from gnomAD population and considered therefore as non-disease causing; in red, variants reported as disease causing or likely disease-causing; in blue, variants of uncertain significance. **B** IGV visualization of RNAseq data from lymphoblastoid cell lines (LCL) of control individuals (CT1-3) and patients with *PQBP1* pathogenic variants (P1-4). **C** RT-qPCR analysis of *UPF3B_S* (normalized on *GAPDH* and *YWHAZ*) in the first serie of LCL including control individuals (CONT, CT1-3, in green) and individuals with pathogenic variants in *PQBP1* (Patho, P1-4, in red) and individuals affected with Fragile-X syndrome (FXS1-3, in yellow) ($n \geq 2$ per cell line), a second set of LCL from control individuals (CT4-6 in green) and individuals with frameshift variant in *PQBP1* (P5, P6 in red), individuals with variants of uncertain significance in *PQBP1* (V1, V1_s, V2) and an additional individual with FXS (FXS4). LCL from individuals with pathogenic variants from the first set (P1-4) were used a calibrator. **D** RT-qPCR analysis of *UPF3B_S* (normalized on *GAPDH* and *YWHAZ*) in blood RNA samples (Paxgene) from individuals with ID without pathogenic variant in *PQBP1* (in green), in individuals with pathogenic or likely pathogenic variants in *PQBP1* p.Arg153fs (P7, P9) and p.Arg243Trp (P8)(in red), individual with VUS in *PQBP1* p.Arg10Pro (V3, in blue), and individuals affected from Fragile-X syndrome (FXS4, FSX5 in yellow) ($n = 1$ Paxgene sample, qPCR triplicates). **E** RT-qPCR analysis of *UPF3B_S* mRNA (normalized on *GAPDH* and *YWHAZ*) in HeLa cells co-transfected with si*Scramble* or si*PQBP1* and WT or mutant *PQBP1* cDNA (WT and benign variant in green, pathogenic variants in red and VUS in blue, $n = 3$ series minimum per condition). Multiple comparisons tests were performed using one-way ANOVA test with Dunnet's correction: ns: not significant; $^{**}p$-value < 0.01; $^{***}p$-value < 0.001; Errors bars represent SEM.

Increase of *UPF3B_S* expression is observed in patients with pathogenic variants in *PQBP1*

In order to test if *UPF3B_S* expression increase observed after transient *PQBP1*-KD in hNSC and fibroblasts is also observed in individuals with Renpenning syndrome, we used lymphoblastoid cell lines (LCL) from individuals carrying variants in *PQBP1* and unaffected individuals (Fig. 3A, Figure S6, Table S1). We performed RNA-Sequencing of LCL from 5 patients carrying pathogenic or

likely pathogenic (P1, P1_s, P2, P3 and P4) versus 3 control individuals (CT1-3), we were able to retrieve the increase of *UPF3B_S* expression (Fig. 3B), as well as the increase of the *PLXNA2* isoform (Figure S3B) observed in hNSC. These increases were found to be more pronounced for patients carrying the truncating recurrent p.Arg153fs variant (*P4*) or the missense variants located in the CTD domain p.Pro244Leu (*P2*) and p.Arg243Trp (*P1, P1_s*) than for the patient with the missense variant located in the WW domain p.Tyr65Cys (*P3*). *UPF3B_S* increase was confirmed by RT-qPCR (Fig. 3C) and was not detected for individuals with another X-linked NDD syndrome, FXS (*FXS1-3*), while it was confirmed in a second set of patients with truncating variants in *PQBP1* (*P5, P6*) (Fig. 3C). As the increase of *UPF3B_S* expression was observed in both patients' LCL and after *PQBP1*-KD in all the cell types analyzed, we intent to use it as a biomarker of *PQPB1* deficiency in order to test the functional consequences of variants in this gene. We tested *UPF3B_S* expression in LCLs from individuals with variants of uncertain significance (VUS) in *PQBP1:* one distal frameshift variant, p.Phe240fs, leading to a protein ten amino acids longer than the wild-type and previously reported by Hu et al. in two brothers with ID with no additional clinical information available [20] and one missense variant p.Arg10Pro located on the N-terminal side of the protein identified in two brothers with severe ID, microcephaly and severe growth retardation, spasticity and additional findings detailed in Table S8. We observed a significant increase of *UPF3B_S* in LCL obtained from two brothers (*V1, V1_s*) carrying the distal frameshift variant, (Fig. 3C). On the contrary, only a moderate increase, not reaching statistical significance, was found for one of the individuals carrying the p.Arg10Pro missense variant (*V2*), similar to what was found for the other variant located on N-terminal side of the protein, p.Tyr65Cys (Fig. 3C).

Increase of *UPF3B_S* expression is a biomarker for variants affecting PQBP1 CTD

As LCL immortalization is not routinely practiced by hospital laboratories, we tested if *UPF3B_S* expression could be detected on mRNA directly extracted from patients' blood. As expected, no expression was detected in control individuals and individuals with FXS, while *UPF3B_S* was found expressed in blood from three individuals with pathogenic variants in *PQBP1* (*P7, P8, P9*) (Fig. 3D). Confirming the results obtained in LCL, only a slight but not significant increase of *UPF3B_S* was observed in blood mRNA from an individual with the p.Arg10Pro variant (*V2*). In order to set up a functional assay which does not require patient material, we performed a complementation test in HeLa cells by co-transfecting *PQBP1* siRNA with optimized siRNA-resistant plasmids containing the wild-type or mutant human *PQBP1* cDNA. We first confirmed that si*PQBP1* transfection increases *UPF3B_S* expression in HeLa cells, while co-transfection with optimized WT *PQBP1* constructs reverts this increase (Fig. 3E, Figure S7). As expected, co-transfection with the *PQBP1* construct containing a variant predicted to be benign (reported in two males from the GnomAD population), p.Arg181Trp, gave results similar to WT. On the contrary, co-transfection with mutant p.Arg153fs failed to revert the *UPF3B_S* increase. Similarly, no complementation was obtained for p.Arg243Trp, p.Pro244Leu and p.Phe240fs mutants, while a partial complementation was observed for p.Tyr65Cys and p.Arg10Pro variants, confirming what we previously observed in LCL (Fig. 3B, C) and suggesting that *UPF3B_S* increase is more pronounced for variants affecting the CTD domain of PQBP1 (truncating variants and missense variants located in this domain) than for variants located in the N-terminal part of the protein. Surprisingly, *UPF3B_S* expression increase was even more pronounced for the p.Arg243Trp, p.Pro244Leu and p.Phe240fs mutants than for p.Arg153fs and the increase was observed even without *PQBP1*-KD, suggesting that these mutants might have a stronger effect than just a loss of *PQBP1*. Therefore, we used this complementation assay to test the effect of an additional variant located in this CTD and reported in literature in an individual with NDD, p.Asp202His [39], and found a significant increase of *UPF3B_S* expression, suggesting a likely pathogenic effect (Fig. 3E). We reviewed the clinical manifestations of the patients analyzed in this study and carrying either a missense variant in the CTD domain, in the N-terminal part, or a frameshift variant. We observed that, independently from their variant location, the different patients present with clinical symptoms which could be consistent with Renpenning syndrome: ID, microcephaly, short stature, language impairment facial dysmorphism including a prominent nose, hypermetropia, ADHD [3, 6] (Table S8). However, patients with the missense variants p.Arg243Trp and p.Pro244Leu seem to present with a milder form of ID, and sometimes borderline or even no ID. An heterogenous IQ illustrating a preserved verbal comprehension ability with a more impaired working memory was measured for *P2* and *P8* for instance, in accordance with what was recently described by others for another individual with the p.Arg243Trp variant [22]. If such mild ID was already previously reported in a few patients with frameshift variants [6], those patients tend in general to present with a more pronounced form of ID. The individuals reported with the missense variants in the WW domain (p.Cys65Tyr and p.Arg10Pro) also have a more severe form of ID and very severe growth retardation [4] (Table S8).

DISCUSSION

In this study, we identified genes and exons differentially expressed after a transient knock-down of *PQBP1* in human neural stem cells (hNSC). The changes in gene expression observed in hNSC, mainly down-regulations, were robust as 80% of them were found significantly deregulated in a second independent hNSC line from another genetic background. Functional annotation of DEG revealed that *PQBP1*-KD affect expression of genes related to neurodegenerative disorders, mRNA regulation and innate immunity, which is highly consistent with the functional roles of PQBP1 previously described by others (review [40]). Identified originally as an interactor of polyQ proteins, PQBP1 is linked to several neurodegenerative disorders. For instance, PQBP1 interacts with proteins involved in cerebellar ataxia type 1 (ATXN1) and Huntington disease (HTT) [7, 11]. PQBP1 was also found to be down-regulated in cortical neurons of individuals with Alzheimer Disease [41]. Moreover, motor neuron degeneration, linked to mitochondrial morphological abnormalities, was identified in *Pqbp1* ko mice [42]. Interestingly several genes related to mitochondrial functions are deregulated after *PQBP1*-KD in hNSC, consistent with what was previously observed in *Pqbp1* cko mice [42], and we observed a decrease of *AMBRA1* expression, a regulator of autophagy leading to a severe form of neurodevelopmental defects when mutated [43]. Several genes encoding transmembrane proteins are down-regulated after *PQBP1*-KD, some of them being important for synapse formation or function (*NRXN2, LRFN4, LRRC4B, SYT2*). Among the genes down-regulated after *PQBP1*-KD, we observed an enrichment in genes involved in other neurodevelopmental disorders such as *CELF2* (expression decreased after *PQBP1*-KD), an RNA binding protein mutated in a neurodevelopmental syndrome with ID and epilepsy [44]. On the other hand, we identified an increase of expression for a non-canonical isoform of *UPF3B*, another X-linked gene involved in different types NDD including ID, autism spectrum disorder and even childhood onset schizophrenia [45, 46]. The increase of this *UPF3B_S* isoform was observed after *PQBP1*-KD in all the cell types analyzed (hNSC, HeLa, fibroblasts) and was also detected from patients' material (mRNA extracted from LCL and blood). Compared to the canonical *UPF3B_L* transcript, this isoform is described to use an alternative transcription initiation site as well as an alternative splicing of

exon 11 (the last exon of the canonical isoform). We therefore showed that *UPF3B_S* expression is a molecular marker for *PQBP1* deficiency, and that effect of variant of uncertain significance (VUS) identified in *PQBP1* could be evaluated from a simple blood RNA extraction.

There is no report about the biological function of this short isoform of *UPF3B*. In a normal context, *UPF3B_S* mRNA appears to be low expressed compared to the canonical isoform, according to the GTEx database. Low expression is detected in different tissues including the brain, and the highest expression was detected in testis. It is noticeable that genital manifestations, and especially microorchidia, are reported for individuals with Renpenning syndrome. While a strong increase of *UPF3B_S* expression was observed for truncating variants or missense variants located in the CTD domain of PQBP1, only a slight increase could be detected for the missense variant p.Tyr65Cys, located in the WW domain, and Pro10Leu. Moreover, several variants affecting the CTD (p.Phe240fs, p.Pro244Leu and p.Arg243Trp) tend to have a stronger effect than *PQBP1* deficiency and lead to *UPF3B_S* increase even when *PQBP1* WT is still expressed (si*Scramble* condition, Fig. 3E). The CTD domain of PQBP1 is known to be involved in the interaction with the splicing factor TXNL4A [11] and it was recently shown that both p.Arg243Trp and p.Pro244Leu variants alter this binding [9, 22]. The p.Tyr65Cys variant, on the contrary, does not affect binding to TXNL4A [9]. We could therefore speculate that pathogenic variants in *PQBP1* have different molecular effects depending of their location on the protein, as *UPF3B_S* expression increase seems to be stronger for variants located affecting CTD domain than for variants located in the N-terminal part of the protein, and we would not recommend using it to test the effect of VUS located on the N-terminal part of the protein. However, if missense variants located in the WW and CTD domains would affect PQBP1 functions in different way, it remains puzzling that the different individuals present clinical symptoms overlapping with Renpenning syndrome. That being said, it is noteworthy the clinical manifestations of the individuals carrying the p.Pro10Leu overlap more strongly with the Golabi-Ito-Hall description of the family with the p.Tyr65Cys variant by Lubs et al. (severe growth retardation, asymmetric face, severe spasticity, etc) [4] than with other individuals with Repenning syndrome. Very recently, a DNA methylation signature was described for individuals with *PQBP1* variants, which could also represent an interesting biomarker for Renpenning syndrome [47]: the methylation profile obtained for the individual with the Tyr65Cys variant seems to show an intermediate profile.

Using immunoprecipitation coupled to mass spectrometry (IP-MS), we confirmed that UPF3B_S can bind to the EJC-protein RBM8A (as predicted by its protein sequence containing RBM8A binding motifs) but not with NMD effectors UPF1 and UPF2. We did not observe NMD dysfunction after *PQBP1*-KD in fibroblasts carrying a premature stop codon (PTC) and we observed no change in expression of natural target of NMD in hNSC. We found that UPF3B isoforms interact with proteins involved in mRNA binding and regulation of translation (ribosomal proteins and translation initiation or elongation factors). Several proteins found to interact with UPF3B are known to be also PQBP1 interactors, such as the translation elongation factor eEF2 [13] or the splicing factor SRRM2. Among the few proteins detected as interacting preferentially with UPF3B_S, some play a role in redox homeostasis or in immune defense against infection. EBV-infected lymphocytes being the second type of cells showing the highest *UPF3B_S* expression, we could speculate that this isoform might play a role in response to infection.

In this study, we showed that *PQBP1*-KD affects the ability of hNSC to proliferate, consistent with what was previously reported by other in non-human neuronal progenitors [26]. Indeed, Ito et al. observed, in nestin-Cre conditional KO mice for *Pqbp1*, which present with reduced head size, a loss of proliferation of neural progenitors probably due to an elongated cell cycle. Interestingly, *Upf3b* KD in mouse neural progenitor cells leads on the contrary to an increase of cell proliferation [48], and patients with loss-of-function variants in *UPF3B* have macrocephaly. Additional experiments would be needed to test if *UPF3B_S* expression increase might contribute to the decrease of hNSC proliferation induced by *PQBP1*-KD and could be linked to Renpenning patients' microcephaly. As *UPF3B_S* is highly expressed in testis, this might also contribute to the microorchidia phenotype of individuals with Renpenning syndrome. Beside head size, additional mirror phenotypes can be observed between Renpenning syndrome and *UPF3B*-related ID, as the short versus tall stature for instance.

In conclusion, we describe here for the first time the consequences of *PQBP1* inactivation in human neural stem cells. We were able to show that cell proliferation is affected, as well as the expression of about fifty genes, with an enrichment of genes involved in other neurodevelopmental disorders. We identified an increase in the expression of a non-canonical isoform of the X-linked NDD gene *UPF3B*. If the function of this isoform remains to be elucidated, its expression represents a biomarker for *PQBP1* deficiency, useful to test VUS and eventually to assess the impact of future therapeutic approaches for Renpenning syndrome.

Web Resources

The URLs for online tools and data presented herein are:

CADD: https://cadd.gs.washington.edu/
ClinVar: http://www.ncbi.nlm.nih.gov/clinvar/
BioGRID: https://thebiogrid.org/
DAVID Tools: https://david.ncifcrf.gov/tools.jsp
Ensembl: https://www.ensembl.org/
GEO: https://www.ncbi.nlm.nih.gov/geo/
GnomAD: http://gnomad.broadinstitute.org/
GTEx : https://gtexportal.org/home/
Integrative Genomics Viewer (IGV): http://www.broadinstitute.org/igv/
OMIM: http://www.omim/org/
SysNDD: https://sysndd.dbmr.unibe.ch/
UCSC: http://genome.ucsc.edu/

DATA AVAILABILITY

Data have been submitted to Gene Expression Omnibus (GSE247739).

REFERENCES

1. Kalscheuer VM, Freude K, Musante L, Jensen LR, Yntema HG, Gécz J, et al. Mutations in the polyglutamine binding protein 1 gene cause X-linked mental retardation. Nat Genet. 2003;35:313–5.
2. Lenski C, Abidi F, Meindl A, Gibson A, Platzer M, Kooy F, et al. Novel truncating mutations in the polyglutamine tract binding protein 1 gene (PQBP1) cause Renpenning syndrome and X-linked mental retardation in another family with microcephaly. Am J Hum Genet. 2004;74:777–80.
3. Kleefstra T, Franken CE, Arens YHJM, Ramakers GJA, Yntema HG, Sistermans EA, et al. Genotype-phenotype studies in three families with mutations in the polyglutamine-binding protein 1 gene (PQBP1). Clin Genet. 2004;66:318–26.
4. Lubs H, Abidi FE, Echeverri R, Holloway L, Meindl A, Stevenson RE, et al. Golabi-Ito-Hall syndrome results from a missense mutation in the WW domain of the PQBP1 gene. J Med Genet. 2006;43:e30.
5. Stevenson RE, Bennett CW, Abidi F, Kleefstra T, Porteous M, Simensen RJ, et al. Renpenning syndrome comes into focus. Am J Med Genet A. 2005;134:415–21.
6. Germanaud D, Rossi M, Bussy G, Gérard D, Hertz-Pannier L, Blanchet P, et al. The Renpenning syndrome spectrum: new clinical insights supported by 13 new PQBP1-mutated males. Clin Genet. 2011;79:225–35.
7. Okazawa H, Rich T, Chang A, Lin X, Waragai M, Kajikawa M, et al. Interaction between mutant ataxin-1 and PQBP-1 affects transcription and cell death. Neuron. 2002;34:701–13.
8. Lee BJ, Cansizoglu AE, Süel KE, Louis TH, Zhang Z, Chook YM. Rules for nuclear localization sequence recognition by karyopherin beta 2. Cell. 2006;126:543–58.

9. Liu X, Dou L-X, Han J, Zhang ZC. The Renpenning syndrome-associated protein PQBP1 facilitates the nuclear import of splicing factor TXNL4A through the karyopherin β2 receptor. J Biol Chem. 2020;295:4093–4100.
10. Wang Q, Moore MJ, Adelmant G, Marto JA, Silver PA. PQBP1, a factor linked to intellectual disability, affects alternative splicing associated with neurite outgrowth. Genes Dev. 2013;27:615–26.
11. Waragai M, Junn E, Kajikawa M, Takeuchi S, Kanazawa I, Shibata M, et al. PQBP-1/Npw38, a nuclear protein binding to the polyglutamine tract, interacts with U5-15kD/dim1p via the carboxyl-terminal domain. Biochem Biophys Res Commun. 2000;273:592–5.
12. Kunde SA, Musante L, Grimme A, Fischer U, Müller E, Wanker EE, et al. The X-chromosome-linked intellectual disability protein PQBP1 is a component of neuronal RNA granules and regulates the appearance of stress granules. Hum Mol Genet. 2011;20:4916–31.
13. Shen Y, Zhang ZC, Cheng S, Liu A, Zuo J, Xia S, et al. PQBP1 promotes translational elongation and regulates hippocampal mGluR-LTD by suppressing eEF2 phosphorylation. Mol Cell. 2021;81:1425–1438.e10.
14. Ikeuchi Y, de la Torre-Ubieta L, Matsuda T, Steen H, Okazawa H, Bonni A. The XLID protein PQBP1 and the GTPase Dynamin 2 define a signaling link that orchestrates ciliary morphogenesis in postmitotic neurons. Cell Rep. 2013;4:879–89.
15. Yoh SM, Schneider M, Seifried J, Soonthornvacharin S, Akleh RE, Olivieri KC, et al. PQBP1 is a proximal sensor of the cGAS-dependent innate response to HIV-1. Cell. 2015;161:1293–305.
16. Jensen LR, Chen W, Moser B, Lipkowitz B, Schroeder C, Musante L, et al. Hybridisation-based resequencing of 17 X-linked intellectual disability genes in 135 patients reveals novel mutations in ATRX, SLC6A8 and PQBP1. Eur J Hum Genet. 2011;19:717–20.
17. Abdel-Salam GMH, Miyake N, Abdel-Hamid MS, Sayed ISM, Gadelhak MI, Ismail SI, et al. Phenotypic and molecular insights into PQBP1-related intellectual disability. Am J Med Genet A. 2018;176:2446–50.
18. Musante L, Kunde S-A, Sulistio TO, Fischer U, Grimme A, Frints SGM, et al. Common pathological mutations in PQBP1 induce nonsense-mediated mRNA decay and enhance exclusion of the mutant exon. Hum Mutat. 2010;31:90–98.
19. Tapia VE, Nicolaescu E, McDonald CB, Musi V, Oka T, Inayoshi Y, et al. Y65C missense mutation in the WW domain of the Golabi-Ito-Hall syndrome protein PQBP1 affects its binding activity and deregulates pre-mRNA splicing. J Biol Chem. 2010;285:19391–401.
20. Hu H, Haas SA, Chelly J, Van Esch H, Raynaud M, de Brouwer APM, et al. X-exome sequencing of 405 unresolved families identifies seven novel intellectual disability genes. Mol Psychiatry. 2016;21:133–48.
21. Redin C, Gérard B, Lauer J, Herenger Y, Muller J, Quartier A, et al. Efficient strategy for the molecular diagnosis of intellectual disability using targeted high-throughput sequencing. J Med Genet 2014;51:724–36.
22. Lopez-Martín, S, Albert, J, Peña Vila-Belda, MDM, Liu, X, Zhang, ZC, Han, J, et al. A mild clinical and neuropsychological phenotype of Renpenning syndrome: A new case report with a maternally inherited PQBP1 missense mutation. Appl Neuropsychol Child. 2022;11:921–7
23. Takahashi K, Yoshina S, Masashi M, Ito W, Inoue T, Shiwaku H, et al. Nematode homologue of PQBP1, a mental retardation causative gene, is involved in lipid metabolism. PLoS One. 2009;4:e4104.
24. Iwasaki Y, Thomsen GH. The splicing factor PQBP1 regulates mesodermal and neural development through FGF signaling. Development. 2014;141:3740–51.
25. Ito H, Yoshimura N, Kurosawa M, Ishii S, Nukina N, Okazawa H. Knockdown of PQBP1 impairs anxiety-related cognition in mouse. Hum Mol Genet. 2009;18:4239–54.
26. Ito H, Shiwaku H, Yoshida C, Homma H, Luo H, Chen X, et al. In utero gene therapy rescues microcephaly caused by Pqbp1-hypofunction in neural stem progenitor cells. Mol Psychiatry. 2015;20:459–71.
27. Tamura T, Sone M, Nakamura Y, Shimamura T, Imoto S, Miyano S, et al. A restricted level of PQBP1 is needed for the best longevity of Drosophila. Neurobiol Aging. 2013;34:356.e11–20.
28. Yang S-S, Ishida T, Fujita K, Nakai Y, Ono T, Okazawa H. PQBP1, an intellectual disability causative gene, affects bone development and growth. Biochem Biophys Res Commun. 2020;523:894–9.
29. Boissart C, Nissan X, Giraud-Triboult K, Peschanski M, Benchoua A. miR-125 potentiates early neural specification of human embryonic stem cells. Development. 2012;139:1247–57.
30. Quartier, A, Chatrousse, L, Redin, C, Keime, C, Haumesser, N, Maglott-Roth, A, et al. Genes and pathways regulated by androgens in human neural cells, potential candidates for the male excess in autism spectrum disorder. Biol Psychiatry. 2018;84:239–52.
31. Kim D, Pertea G, Trapnell C, Pimentel H, Kelley R, Salzberg SL. TopHat2: accurate alignment of transcriptomes in the presence of insertions, deletions and gene fusions. Genome Biol. 2013;14:R36.
32. Langmead B, Salzberg SL. Fast gapped-read alignment with Bowtie 2. Nat Methods. 2012;9:357–9.
33. Anders S, Pyl PT, Huber W. HTSeq-a Python framework to work with high-throughput sequencing data. Bioinformatics. 2015;31:166–9.
34. Benjamini, Y. Controlling the false discovery rate: a practical and powerful approach to multiple testing. Journal of the Royal Statistical Society B. 1995;57:289–300.
35. Anders S, Reyes A, Huber W. Detecting differential usage of exons from RNA-seq data. Genome Res. 2012;22:2008–17.
36. Mattioli F, Isidor B, Abdul-Rahman O, Gunter A, Huang L, Kumar R, et al. Clinical and functional characterization of recurrent missense variants implicated in THOC6-related intellectual disability. Hum Mol Genet 2019;28:952–60.
37. Nickless A, Bailis JM, You Z. Control of gene expression through the nonsense-mediated RNA decay pathway. Cell Biosci. 2017;7:26.
38. Courraud, J, Chater-Diehl, E, Durand, B, Vincent, M, del Mar Muniz Moreno, M, Boujelbene, I, et al. Integrative approach to interpret DYRK1A variants, leading to a frequent neurodevelopmental disorder. Genet Med. 2021;23:2150–9.
39. Morgan A, Gandin I, Belcaro C, Palumbo P, Palumbo O, Biamino E, et al. Target sequencing approach intended to discover new mutations in non-syndromic intellectual disability. Mutat Res. 2015;781:32–36.
40. Tanaka H, Okazawa H. PQBP1: The key to intellectual disability, neurodegenerative diseases, and innate immunity. Int J Mol Sci. 2022;23:6227.
41. Tanaka H, Kondo K, Chen X, Homma H, Tagawa K, Kerever A, et al. The intellectual disability gene PQBP1 rescues Alzheimer's disease pathology. Mol Psychiatry. 2018;23:2090–110.
42. Marubuchi S, Wada YI, Okuda T, Hara Y, Qi ML, Hoshino M, et al. Polyglutamine tract-binding protein-1 dysfunction induces cell death of neurons through mitochondrial stress. J Neurochem. 2005;95:858–70.
43. Ye J, Tong Y, Lv J, Peng R, Chen S, Kuang L, et al. Rare mutations in the autophagy-regulating gene AMBRA1 contribute to human neural tube defects. Hum Mutat. 2020;41:1383–93.
44. Itai T, Hamanaka K, Sasaki K, Wagner M, Kotzaeridou U, Brösse I, et al. De novo variants in CELF2 that disrupt the nuclear localization signal cause developmental and epileptic encephalopathy. Hum Mutat. 2021;42:66–76.
45. Tarpey PS, Raymond FL, Nguyen LS, Rodriguez J, Hackett A, Vandeleur L, et al. Mutations in UPF3B, a member of the nonsense-mediated mRNA decay complex, cause syndromic and nonsyndromic mental retardation. Nat Genet. 2007;39:1127–33.
46. Addington AM, Gauthier J, Piton A, Hamdan FF, Raymond A, Gogtay N, et al. A novel frameshift mutation in UPF3B identified in brothers affected with childhood onset schizophrenia and autism spectrum disorders. Mol Psychiatry. 2011;16:238–9.
47. Haghshenas, S, Foroutan, A, Bhai, P, Levy, MA, Relator, R, Kerkhof, J, et al. Identification of a DNA methylation signature for Renpenning syndrome (RENS1), a spliceopathy. Eur J Hum Genet. 2023;31:879–86.
48. Jolly LA, Homan CC, Jacob R, Barry S, Gecz J. The UPF3B gene, implicated in intellectual disability, autism, ADHD and childhood onset schizophrenia regulates neural progenitor cell behaviour and neuronal outgrowth. Hum Mol Genet. 2013;22:4673–87.

ACKNOWLEDGEMENTS

The authors would like to thank the families for their participation and support. The authors also thank the Agence de Biomédecine, Fondation APLM for financial support, as well as Besançon Hospital and University for Camille Engel's fellowship. We also thank the GenomEast sequencing platform for performing RNASeq and for their help in data analysis, as well as Bastien Morlet from the Mass spectrometry platform and Anne Maglott from the high-throughput screening platform. We thank Camille Dourlens for her participation to the project as well as Josef Gecz, Frederic Laumonnier, Renaud Touraine and David Germanaud for scientific discussion and advice.

AUTHOR CONTRIBUTIONS

Experiment realization: JC, CE, AQ, ND, UH, AP; Acquisition of molecular and clinical genetic data: CE, AS, EBB, EG, LVM, MR, GL, PE, FB, BGD, IA, VMK, AP, JLM; Data analysis : JC, CE, AQ, ND, UH, DP; Writing and editing manuscript: JC, VMK, AP, JLM, Conceptualization and supervision: AP; Funding acquisition: AP, JLM.

COMPETING INTERESTS

The authors declare no competing interests.

ETHICS

Individuals were referred by clinical geneticists for genetic testing as part of routine clinical care. All patients enrolled and/or their legal representative have signed informed consent for research use and authorization for publication. IRB approval was obtained from the Ethics Committee of the Strasbourg University Hospital (CCPPRB) as well as from local institutions.

ADDITIONAL INFORMATION

Supplementary information The online version contains supplementary material available at https://doi.org/10.1038/s41380-023-02323-5.

Correspondence and requests for materials should be addressed to Amélie Piton.